AFRL-RX-WP-TP-2010-4077

A COMBINED THERMODYNAMIC/KINETIC MODELING APPROACH TO PREDICT SiC RECESSION DUE TO SiO_2 SCALE VOLATILITY UNDER COMBUSTION ENVIRONMENTS (PREPRINT)

F. Zhang, S.-L. Chen, and W.-S. Cao

CompuTherm, LLC

C. Zhang and Y. A. Chang

University of Wisconsin-Madison

J. Simmons

Metals Branch
Metals, Ceramics & NDE Division

FEBRUARY 2010

AIR FORCE RESEARCH LABORATORY
MATERIALS AND MANUFACTURING DIRECTORATE
WRIGHT-PATTERSON AIR FORCE BASE, OH 45433-7750
AIR FORCE MATERIEL COMMAND
UNITED STATES AIR FORCE

REPORT DOCUMENTATION PAGE

Form Approved
OMB No. 0704-0188

1. REPORT DATE *(DD-MM-YY)*	2. REPORT TYPE	3. DATES COVERED *(From - To)*
January 2010	Journal Article Preprint	01 February 2010 – 01 February 2010

4. TITLE AND SUBTITLE

A COMBINED THERMODYNAMIC/KINETIC MODELING APPROACH TO PREDICT SiC RECESSION DUE TO SiO_2 SCALE VOLATILITY UNDER COMBUSTION ENVIRONMENTS (PREPRINT)

5a. CONTRACT NUMBER
In-house

5b. GRANT NUMBER

5c. PROGRAM ELEMENT NUMBER
62102F

6. AUTHOR(S)

F. Zhang, S.-L. Chen, and W.-S. Cao (CompuTherm, LLC)
C. Zhang and Y. A. Chang (University of Wisconsin-Madison)
J. Simmons (AFRL/RXLMD)

5d. PROJECT NUMBER
4347

5e. TASK NUMBER
RG

5f. WORK UNIT NUMBER
M02R2000

7. PERFORMING ORGANIZATION NAME(S) AND ADDRESS(ES)

CompuTherm, LLC
Madison, WI 53719

University of Wisconsin-Madison
Department of Materials Science and Engineering
Madison, WI 53706

Metals Branch (AFRL/RXLMD)
Metals, Ceramics & NDE Division
Materials and Manufacturing Directorate
WPAFB, OH 45433-7750
Air Force Materiel Command, United States Air Force

8. PERFORMING ORGANIZATION REPORT NUMBER
AFRL-RX-WP-TP-2010-4077

9. SPONSORING/MONITORING AGENCY NAME(S) AND ADDRESS(ES)

Air Force Research Laboratory
Materials and Manufacturing Directorate
Wright-Patterson Air Force Base, OH 45433-7750
Air Force Materiel Command
United States Air Force

10. SPONSORING/MONITORING AGENCY ACRONYM(S)
AFRL/RX

11. SPONSORING/MONITORING AGENCY REPORT NUMBER(S)
AFRL-RX-WP-TP-2010-4077

12. DISTRIBUTION/AVAILABILITY STATEMENT
Approved for public release; distribution unlimited.

13. SUPPLEMENTARY NOTES
Journal article submitted to *Acta Materialia*. PAO Case Number: 88ABW-2009-5144; Clearance Date: 11 Dec 2009. Paper contains color.

14. ABSTRACT

A computational approach, which targets on the prediction of SiC recession caused by SiO_2 scale volatility under combustion environments, was developed in this study. In this approach, thermodynamic calculation was integrated with a gaseous-diffusion model to calculate the fluxes of volatile species, such as SiO(g), $Si(OH)_4$(g), $SiO(OH)_2$(g), and SiO(OH)(g), produced by the reaction of SiO_2 scale with the combustion air. The resulted weight loss of SiC was then calculated under a variety of combustion environments. The benefit of using environmental barrier coating (EBC) in the protection of SiC from recession was demonstrated by the calculation. It is shown that the weight loss of SiC-based ceramics could be significantly reduced when EBCs, such as mullite ($Al_6Si_2O_{13}$ or written as $3Al_2O_3$•$2SiO_2$) or $SrAS_2$ (SrO•Al_2O_3•$2SiO_2$), are used. The effects of combustion conditions, such as temperature and total pressure, on the volatility of SiO_2 scale were also discussed.

15. SUBJECT TERMS
thermodynamic modeling, SiC recession, SiO_2 scale volatility, environmental barrier coating

16. SECURITY CLASSIFICATION OF:			17. LIMITATION OF ABSTRACT:	18. NUMBER OF PAGES	19a. NAME OF RESPONSIBLE PERSON (Monitor)
a. REPORT	b. ABSTRACT	c. THIS PAGE			Sheldon L. Semiatin
Unclassified	Unclassified	Unclassified	SAR	48	19b. TELEPHONE NUMBER *(Include Area Code)* N/A

Standard Form 298 (Rev. 8-98)
Prescribed by ANSI Std. Z39-18

A Combined Thermodynamic/Kinetic Modeling Approach to Predict SiC Recession due to SiO2 Scale Volatility under Combustion Environments

Submitted to:

Acta Materialia

Authors:

F. Zhang[a], C. Zhang[b], S.-L. Chen[a], W.-S. Cao[a], J. Simmons[c], and Y. A. Chang[b*]

[a] CompuTherm, LLC, Madison, WI 53719

[b] Department of Materials Science and Engineering, University of Wisconsin-Madison, Madison, WI 53706

[c] Air Force Research Lab, WPAFB, OH 45433

[*] Corresponding Author

Y. Austin Chang

Department of Materials Science and Engineering, University of Wisconsin-Madison,

1509 University Ave., Madison, WI 53706

Tel: 608-262-0389

Email: Chang@engr.wisc.edu or changy@cae.wisc.edu

Key Words: Thermodynamic Modeling, SiC Recession, SiO_2 Scale Volatility, Environmental Barrier Coating

A Combined Thermodynamic/Kinetic Modeling Approach to Predict SiC Recession due to SiO2 Scale Volatility under Combustion Environments

ABSTRACT

A computational approach, which targets on the prediction of SiC recession caused by SiO_2 scale volatility under combustion environments, was developed in this study. In this approach, thermodynamic calculation was integrated with a gaseous-diffusion model to calculate the fluxes of volatile species, such as SiO(g), $Si(OH)_4$(g), $SiO(OH)_2$(g), and SiO(OH)(g), produced by the reaction of SiO_2 scale with the combustion air. The resulted weight loss of SiC was then calculated under a variety of combustion environments. The benefit of using environmental barrier coating (EBC) in the protection of SiC from recession was demonstrated by the calculation. It is shown that the weight loss of SiC-based ceramics could be significantly reduced when EBCs, such as mullite ($Al_6Si_2O_{13}$ or written as $3Al_2O_3{\cdot}2SiO_2$) or $SrAS_2$ ($SrO{\cdot}Al_2O_3{\cdot}2SiO_2$), are used. The effects of combustion conditions, such as temperature and total pressure, on the volatility of SiO_2 scale were also discussed.

1. INTRODUCTION

Ceramic matrix composites (CMCs), which combine reinforcing ceramic phases with a ceramic matrix, create materials with superior properties. Si-based ceramics, such as silicon carbide (SiC) fiber-reinforced SiC ceramic matrix composites (SiC/SiC CMCs),

are potential candidates for turbine engine applications owing to their high temperature strength and durability, as well as low density. However, their usage as turbine engine hot-section components is stumbled due to their lack of environmental durability in high velocity combustion environments. The silica scale (SiO_2), which is responsible for the excellent high temperature oxidation resistance in dry air, reacts with water vapor and forms gaseous silicon oxide and hydroxide species [1] under combustion environments. The volatilization of these species results in further oxidation of SiC and recession of Si-based ceramics. To minimize the recession of Si-based ceramics, environmental barrier coatings (EBCs) have been developed to prevent silica scale from reacting with the combustion gases.

The first generation of EBCs is based on mullite ($Al_6Si_2O_{13}$ or written as $3Al_2O_3{\cdot}2SiO_2$) due to its low coefficient of thermal expansion (CTE), excellent chemical compatibility with Si-based ceramics, and good adherence [2-4]. One major issue with the mullite coating is its relatively high silica activity (~0.5) and the resulted selective volatilization of silica by water vapor. To overcome the recession of mullite, water vapor resistant, such as yttria-stabilized zirconia (YSZ), was used as top coat. However, one critical weakness of YSZ is its large CTE, twice that of SiC or mullite. Under long-term exposure to thermal cycling, the CTE mismatch causes severe cracking and delamination, and leads to premature EBC failure [1]. For the second generation of EBCs, the YSZ top coat was replaced by the BSAS [$(1\text{-}x)BaO\text{-}xSrO\text{-}Al_2O_3\text{-}2SiO_2$] family materials. Current EBCs usually contain three layers, the Si-bond coat, the mullite intermediate coat, and the BSAS top coat. One of the research focuses is to identify new top coats that have higher

temperature capability and chemical/mechanical compatibility with the mullite intermediate coat.

To accelerate the development of advanced coating materials for SiC-based ceramics, integration of computational modeling approach with key experiments is essential. The computational approach is used to identify the potential materials, while experiments are used to validate the prediction. It is our ultimate goal to develop a modeling tool that can be used to predict the phase stability and compatibility of EBCs with the SiC-based substrate, the durability and high temperature capability of selected EBCs, the volatility of the SiO_2 scale, and the recession of SiC-based ceramic materials under a variety of combustion environments. The focus of the present paper is to calculate the volatility of the SiO_2 scale and the weight loss of SiC at different combustion conditions and understand the protective roles of the two selected EBCs. A thermodynamic database, which compiles the Gibbs energies of the gas phase and the condensed phases of the silica-oxides system, was used to calculate the equilibrium between the EBCs and the combustion gas. The gaseous-diffusion model proposed by Opila *et al.* [5, 6] was used to calculate the volatility of the SiO_2 scale, and will be briefly reviewed in Section 2.1. The significant contribution of this paper is that multi-component, multi-phase equilibrium calculation is directly coupled with the gaseous-diffusion model to calculate the equilibrium partial pressures and the fluxes of volatile silicon species given a combustion condition. More importantly, the thermodynamic database of the silica-oxides system allows us to have an insight view on how a selected EBC can effectively protect SiC from recession through the calculation of the activity of SiO_2, as will be demonstrated in

Section 3.2. The purpose of this work is not to validate the gaseous-diffusion model proposed by Opila *et al.* [5, 6], while the effects of combustion condition, such as temperature, total pressure, and the equivalent factor, will be discussed in Section 3.3. Limitations of the approach will be discussed in Section 3.4, and conclusions be presented in Section 4.

2. THERORY AND APPROACH

2.1 Volatile Kinetics of SiO_2

SiC is thermodynamically unstable in an oxidizing environment and forms an outer scale of SiO_2. As presented in the paper by Opila *et al.* [5], in a combustion environment containing O_2, CO_2, and H_2O, SiC can be oxidized by any or all of the following reactions:

$$SiC + \frac{3}{2}O_2(g) = SiO_2 + CO(g) \quad (1)$$

$$SiC + 3CO_2(g) = SiO_2 + 4CO(g) \quad (2)$$

$$SiC + 3H_2O(g) = SiO_2 + CO(g) + 3H_2(g) \quad (3)$$

Due to the slow growth rate, SiO_2 forms a protective layer for the SiC under oxidizing environment. However, under a reducing environment, or in an oxidizing/reducing gas mixture, such as H_2O/H_2 or CO_2/CO mixtures, the SiO_2 can be reduced to form volatile SiO(g) by the following reactions:

$$SiO_2 + H_2(g) = SiO(g) + H_2O(g) \quad (4)$$

$$SiO_2 + CO(g) = SiO(g) + CO_2(g) \quad (5)$$

Similarly, in water-vapor containing environments, SiO_2 scale may react with H_2O(g) to form volatile hydroxides or oxyhydroxides by one of the following reactions [5]:

$$SiO_2 + H_2O(g) = SiO(OH)_2(g) \quad (6)$$

$$SiO_2 + 2H_2O(g) = Si(OH)_4(g) \quad (7)$$

$$2SiO_2 + 3H_2O(g) = Si_2O(OH)_6(g) \quad (8)$$

$$SiO_2 + \frac{1}{2}H_2O(g) = SiO(OH)(g) + \frac{1}{4}O_2(g) \quad (9)$$

$$2SiO_2 + 3H_2O(g) = Si_2(OH)_6(g) + \frac{1}{2}O_2(g) \quad (10)$$

It is seen from Equations (4)–(10) that SiO_2 volatility is attributed primarily to the formation of gaseous species, such as SiO(g), $Si(OH)_4$(g), $Si(OH)_x$(g), and $SiO(OH)_x$(g). Notice that, under a particular combustion environment, only a few of the above chemical reactions are predominant. The partial pressure of each gas species can be calculated when the system reaches equilibrium. Taking the reaction shown in Eq. (7) as an example, we have:

$$\frac{P_{Si(OH)_4(g)}}{P^2_{H_2O(g)} a_{SiO_2}} = \exp(\frac{-\Delta G^\circ_f}{RT}) \quad (11)$$

Where ΔG_f° is the Gibbs energy change of the chemical reaction, R the gas constant, and T the temperature in Kelvin; $P_{Si(OH)_4(g)}$, and $P_{H_2O(g)}$ are the partial pressures of $Si(OH)_4$(g) and H_2O(g), respectively, and a_{SiO_2} the activity of SiO_2 in the scale. It should be pointed out that, the equilibrium partial pressures of these volatile species, such as $Si(OH)_4$(g) in the above equation, are directly related to the activity of SiO_2. Apparently, low a_{SiO_2} will suppress the chemical reactions going to the right hand side, reduce the equilibrium partial pressures of volatile species, and consequently limit the volatilization of SiO_2. This point will be elaborated in Section 3: RESULTS and DISCUSSIONS.

While thermodynamics can only provide equilibrium partial pressures of these gas species, the gaseous-diffusion model developed by Opila and colleagues [5, 7] is used to calculate their fluxes in this study. In their model, the fluxes of volatile silicon oxides, hydroxides, or oxyhydroxides are controlled by diffusion through a gaseous boundary layer. In laminar-flow conditions, the following equation [8] is used to calculate the boundary-layer-limited flux of species *i*:

$$J_i = 0.664 Re^{\frac{1}{2}} Sc^{\frac{1}{3}} \frac{D\rho_{V_i}}{L} \tag{12}$$

where J_i is the mass flux of volatile species *i*, such as SiO(g) and $Si(OH)_4$(g), *Re* the Reynolds number, *Sc* the Schmidt number, *D* the interdiffusion coefficient of the volatile species in the boundary-layer combustion gas, ρ_{V_i} the density of the volatile species *i* at

the solid/gas interface, and L the characteristic length of the test specimen parallel to the direction of the gas flow. Expanding the Reynolds and Schmidt numbers results in,

$$J_i = 0.664(\frac{\rho \nu L}{\eta})^{\frac{1}{2}}(\frac{\eta}{\rho D})^{\frac{1}{3}}\frac{D\rho_{V_i}}{L} \tag{13}$$

where ρ is the density of the boundary-layer combustion gas, ν the linear gas velocity, and η the gas viscosity. In this equation, L and ν are experimental inputs, η can be found in the literature [9], and D can be calculated by the Chapman-Enskog equation [10]. The gas densities, ρ and ρ_{V_i} are determined by the partial pressures of the gaseous species. Given the combustion gas environment, temperature and pressure, the partial pressures of the combustion gas species: O_2, H_2, H_2O, CO, CO_2, N_2, as well as those volatile species at the solid/gas interface: SiO(g), $Si(OH)_4$(g), etc., can be calculated using the thermodynamic database for the gas species. The gas densities ρ and ρ_{V_i} can then be calculated from the equation of state for an ideal gas:

$$\rho_{V_i} = \frac{P_i M_i}{RT} \qquad (i = SiO(g), Si(OH)_4, etc.) \tag{14}$$

$$\rho = \sum_j \frac{P_j M_j}{RT} \qquad (j = O_2(g), H_2O, N_2, etc.) \tag{15}$$

where P_i and P_j represent the partial pressures of the volatile silicon species and the gas species in the combustion environment, respectively, M_i and M_j are the corresponding atomic weights, R is the gas constant and T temperature. By using the partial pressures of

gaseous species obtained from thermodynamic calculation and Eqs. (13)-(15), the fluxes of the volatile silicon species can be calculated. These values can then be used to calculate the weight loss of SiC.

2.2 Thermodynamic Database for the Gas Species and the EBC Systems

In order to calculate the partial pressure of each gas species and the fluxes of volatile species, thermodynamic database for the gas species must be developed. The gas species considered in this study are those in the combustion environment, such as O_2, H_2, CO, CO_2, H_2O, and N_2, and the products due to the reaction of SiO_2 with the combustion environments, such as SiO(g), $Si(OH)_4$(g), SiO(OH)(g), $SiO(OH)_2$(g). Gibbs energy functions for these species were developed based on the published thermochemical data in the literatures [5, 11]. The Gibbs energy of the gas phase is described by the following equation:

$$G = \sum_{s=1}^{n} y_s G_s^\circ + RT \sum_{s=1}^{n} y_s \ln(y_s \gamma_s P) = \sum_{s=1}^{n} y_s [G_s^\circ + RT \ln(y_s \gamma_s) + RT \ln P] \tag{16}$$

where P is the total external pressure in bar, G_s° is the Gibbs energy of the species s at the reference pressure of one bar, n is the number of species and y_s is the molar fraction of the species s in the gas phase. The fugacity coefficient, γ_s, is used to describe the non-ideal gas, which is unity for an ideal gas.

As has been pointed out in Section 2.1, the equilibrium partial pressures of volatile species in the gas phase are directly related to the activity of SiO_2 in the scale. The activity of SiO_2 is unity when SiC is directly exposed to the combustion environment and SiO_2 scale builds up on the surface. This is not true when an environment barrier coating (EBC) is used, in which case the activity of SiO_2 should be calculated using the thermodynamic database of the EBC system. In this study, thermodynamic database for the SrO-Al_2O_3-SiO_2 pseudo-ternary system developed by Zhang *et al.* [12] was used to calculate the activity of SiO_2 for mullite ($Al_6Si_2O_{13}$ or written as $3Al_2O_3{\cdot}2SiO_2$) or $SrAS_2$ ($SrO{\cdot}Al_2O_3{\cdot}2SiO_2$) coatings. Details on the thermodynamic models used to describe the phases in the SrO-Al_2O_3-SiO_2 system, as well as database development, will be published in a separate paper [12]. It should be pointed out that $SrO{\cdot}Al_2O_3{\cdot}2SiO_2$, which was refereed to as SAS by Lee *et al.* [1], is abbreviated as $SrAS_2$. This is to distinguish it from the other two ternary compounds in this pseudo-ternary system as will be discussed in Section 3.2.

2.3 Software Modules for Calculating Complicated Phase Equilibria, Gas-Solid Reaction and Volatilization of SiO_2

Software package, an essential part of this study, is used to deal with complicated phase equilibria, gas-solid reaction and SiO_2 volatilization. In this study, all the functions are built upon *Pandat* [13], a software package for multi-component phase diagram calculations. The unique feature of *Pandat* is its ability to automatically find the stable phase equilibrium in a multi-component, multi-phase system. The gas-solid reaction

module is used to find the equilibrium between the gas phase and the EBC system. Figure 1 is a flow chart showing the connection between different modules of the software and the thermodynamic databases. Thermodynamic database for the EBC system provides the software with Gibbs energy functions of the condensed phases to find the phase equilibria in the EBC system. The calculated phase stability and activity data, as well as the Gibbs energies of gas species, are inputs for the gas-solid reaction module. The equilibrium partial pressures of gas species calculated from the gas-solid reaction module are then used by the kinetic module for calculating the fluxes of the volatile silicon oxide, hydroxide, and oxyhydroxide species.

3. RESULTS AND DISCUSSIONS

3.1 SiC Weight Loss When Directly Exposed to the Combustion Environments

Robinson and colleagues [6] carried out experimental study on the SiC recession caused by SiO_2 scale volatility under combustion conditions. In their study, SiC coupons were directly exposed to the combustion environments. The SiO_2 was first formed on the sample surface, and then volatilized due to its reaction with combustion air to form volatile species, such as SiO, $Si(OH)_4$, $SiO(OH)_2$, SiO(OH). The process follows paralinear kinetics, i.e. a simultaneous parabolic scale growth, concurrent with linear volatilization of the scale. However, steady state was quickly established, and linear weight loss of SiC was measured in their study. Table I lists the experimental conditions of their experiments. In this table, T, P and V_g represent the temperature, total pressure,

and gas velocity of the combustion air. The equivalent ratio, represented by ϕ, is defined as the fuel-to-air ratio with the total hydrocarbon (fuel) content normalized to the amount of oxygen. At $\phi = 1$, combustion results in complete consumption of fuel and oxygen. For the case of fuel lean, i.e., $\phi < 1$, the combustion air will contain N_2, H_2O, CO_2, and O_2 as major species; while for the case of fuel rich, i.e., $\phi > 1$, the combustion air will contain N_2, H_2O, CO_2, H_2 and CO.

The calculation condition used in this work is listed in Table II, and the calculated SiC loss is compared with the experimental data of Robinson's work [6]. Figure 2 compares the calculated and experimentally measured SiC weight loss rate under fuel lean condition (refer to Tables I and II). It shows a very good agreement at low temperature range (below 1500^{o}C), while the calculated weight loss tends to be higher than that determined by Robinson etc.[6] at higher temperature (above 1500^{o}C). Figure 3 shows a comparison between the calculated and experimentally measured SiC weight loss rate under fuel rich condition (refer to Tables I and II), and less satisfactory results are obtained. The calculated weight loss rates are lower than those determined by experiments, which is probably due to the formation of other volatile gas species, such as $Si(OH)_6$. Due to the lack of thermochemical data for this species, its Gibbs energy is unknown and therefore not considered in the current thermodynamic database. Figure 4, which compares the calculated and experimentally measured SiC weight loss at two pressures, indicates that the model prediction works well at different pressures under fuel lean condition. In fact, the calculation for the higher pressure (10atm) agrees with the experimental measurements better, even for high temperature. The effects of temperature

and pressure on the weight loss of SiC are shown in Figure 5 and Figure 6. It is apparent that higher temperature and/or higher pressure of the combustion air lead to heavier SiC weight loss.

3.2 SiC Weight Loss When Mullite or $SrAS_2$ Coating is used

As has been pointed out, the fluxes of volatile species and the weight loss of SiC are directly related to the activity of SiO_2. It is seen from equation (11) that low a_{SiO_2} suppresses the chemical reactions going to the right hand side (equation (7)), and consequently reduces the volatility of SiO_2. For the case discussed in Section 3.1, bare SiC substrate directly exposed to the combustion environment was first oxidized to form SiO_2 scale, therefore $a_{SiO_2}=1$ in the scale. In this section, we will demonstrate that SiC recession rate is reduced when mullite or $SrAS_2$ is used as coating due to the lower activity of SiO_2 ($a_{SiO_2}<1$) in the EBC.

Mullite ($3Al_2O_3 \cdot 2SiO_2$) forms in the SiO_2–Al_2O_3 pseudo-binary system as shown in Figure 7. The activity of SiO_2 is calculated along this pseudo-binary at 1500K and plotted in Figure 8. As can be seen, a_{SiO_2} is 1 in the SiO_2+Mullite two-phase field, and decreases from 1 to 0.506 in the single mullite field and keeps constant 0.506 in the Mullite+Al_2O_3 two-phase field. Figure 9 shows the activity of SiO_2 in mullite as a function of temperature. This plot does not make sense at first sight since the activity of SiO_2 decreases as temperature increases. This figure needs to be understood in combination with Figure 7 and Figure 8 together. It is seen from Figure 7 that mullite has a certain

range of homogeneity and its phase boundary is tilted. Figure 8 indicates that the activity of SiO_2 changes dramatically within the mullite single phase region. It is in fact not suitable to compare the activity of SiO_2 at different temperatures at the stoichiometric composition of mullite ($Al_6Si_2O_{13}$) since this composition may locate in the SiO_2+Mullite two-phase field, single mullite phase field, or Mullite+Al_2O_3 two-phase field depending on the temperature. The activity showed in Figure 9 is actually the activity of SiO_2 in the Mullite+Al_2O_3 two-phase field, or the activity of SiO_2 following the phase boundary of mullite in equilibrium with Al_2O_3, which is tilted away from SiO_2 at higher temperature. This is why the activity of SiO_2 decreases as the temperature increases.

Figure 10 is the isothermal section of the SrO-Al_2O_3-SiO_2 pseudo-ternary at 1350^{o}C. The activity of SiO_2 with $SrAS_2$ ($SrO{\cdot}Al_2O_3{\cdot}2SiO_2$) composition is calculated as a function of temperature as shown in Figure 11. It is seen from Figure 9 and Figure 11 that the activity of SiO_2 varies from 0.53 to 0.43 in mullite, and from 0.04 to 0.15 in $SrAS_2$ in the temperature range of 1400K to 1800K. $SrAS_2$ is therefore expected to better protect SiO_2 from volatilization and SiC recession due to the lower activity of SiO_2 in it. This point is clearly shown in Figure 12, in which the SiC weight loss rate is calculated as a function of temperature under the combustion condition of fuel lean at 6 atm. These calculations indicate that SiC suffers significant weight loss when it is directly exposed to the combustion environment, mullite coating helps to reduce the SiC weight loss by about 50%, and $SrAS_2$ coating helps further preventing SiC from recession.

In the paper of Lee *et al*. [1], experimental measurements were carried out to determine the weight loss of SiC when the BSAS family coatings were used. The $SrAS_2$ (refereed to as SAS in Lee's paper) coated SiC samples were exposed to 50% H_2O-balance O_2 flowing at 4.4cm/s at 1500^{o}C. The total pressure of H_2O and O_2 was 1 atm. The activity of SiO_2 for $SrAS_2$ ($SrO{\cdot}Al_2O_3{\cdot}2SiO_2$) is calculated to be 0.145 at 1500^{o}C, and the calculated SiC weight loss as a function of time is shown in Figure 13. The experimentally determined weight loss by Lee *et al*. [1] were also plotted on the figure for comparison. Even though the calculation over predicted the weight loss by about 20%, fairly good agreement is obtained.

Mullite and $SrAS_2$ were selected in the calculation to demonstrate their protective roles as EBCs due to the fact that these two materials have been studied experimentally for such a purpose. In addition to $SrAS_2$, there are two other compounds: Sr_2AS ($2SrO{\cdot}Al_2O_3{\cdot}SiO_2$) and $Sr_6A_9S_2$ ($6SrO{\cdot}9Al_2O_3{\cdot}2SiO_2$) in the SrO-Al_2O_3-SiO_2 pseudo-ternary system as shown in Figure 10. To the best of our knowledge, their potential applications as EBCs for SiC have not been studied experimentally. It would be interesting to see if they have such a potential from a thermodynamic point of view. The activity of SiO_2 in both Sr_2AS and $Sr_6A_9S_2$ were calculated as a function of temperature and compared with that of $SrAS_2$ as shown in Figure 14. As it is seen, both Sr_2AS and $Sr_6A_9S_2$ show lower activities of SiO_2, which indicates that they should be more effective in protecting SiO_2 from volatilization and SiC from recession. This is especially true for Sr_2AS, in which the activity of SiO_2 is several orders of magnitude lower than that of $SrAS_2$. However, it should also be pointed out that this conclusion is reached only in view of their activities.

To develop good coating materials, their chemical compatibility with Si-based ceramics, coefficient of thermal expansion (CTE), and adherence need to be addressed as well. Nevertheless, Sr_2AS and $Sr_6A_9S_2$ identified by the thermodynamic calculations of this study are worthwhile for future experimental investigation.

3.3 Effects of the Equivalent Factor, Temperature, Pressure and Activity of SiO_2 on the Partial Pressures of Gas Species

In order to understand the volatilization of SiO_2 and the recession of SiC-based ceramics under different combustion environments, it is essential to know how the partial pressure of each gas species changes with the equivalent ratio ϕ, temperature, pressure and activity of SiO_2. In this section, we will plot the calculated partial pressures of gas species as a function of ϕ at different temperature, total pressure and activity of SiO_2. Figure 15 is the one for the combustion condition at 1200^oC with a total pressure of 6atm. Figure 15 (a) shows the distribution of every gas species in the combustion air, while Figure 15 (b) is for the volatile silicon oxide, hydroxides, oxyhydroxides due to the reaction of SiO_2 with the combustion air. As has been discussed in Section 3.1, the equivalent ratio (ϕ) is defined as the fuel-to-air ratio with the total hydrocarbon (fuel) content normalized to the amount of oxygen. It is fuel lean when the equivalent ratio is less than one and fuel rich when the equivalent ratio is greater than one. As is seen from Figure 15 (a), the concentrations of N_2, H_2O, and CO_2 remain almost constants at both fuel lean and fuel rich conditions. O_2 is one of the major species at fuel lean condition, while it is almost completely consumed at fuel rich condition. On the other hand, the existence of H_2 and

CO is negligible at fuel lean, but they become the major species at fuel rich condition. The partial pressures of O_2, H_2, and CO go through dramatic change near the area where the equivalent ratio is one. Although the concentrations of these species vary slightly due to the change of temperature and total pressure, their distributions as a function of ϕ keep the same trend as that shown in Figure 15 (a). Similar plots for the distribution of these species at different temperatures and pressures, therefore, will not be repeated in this paper. In the following discussions, we will focus on the variation of the volatile species: SiO, $Si(OH)_4$, $SiO(OH)_2$ and SiO(OH), since they are the ones that directly contribute to the volatility of SiO_2.

Figure 16 (a) shows the partial pressure change of the volatile species when the total pressure jumps from 6 atm to 12 atm. Figure 16 (b) is the enlarged plot of the top portion of Figure 16 (a). It is seen from these two figures that the partial pressure change of SiO and SiO(OH) is negligible, while the partial pressure of $Si(OH)_4$ increases by five folds, and $SiO(OH)_2$ by three folds as the total pressure increases from 6 atm to 12 atm. This is consistent with Figure 6 which shows that the total weight loss of SiC is proportional to the total pressure. Figure 17 shows the partial pressure change of these species when the temperature changes from 1200^{o}C to 1500^{o}C. Temperature seems to have a big impact on the partial pressures of these species. The partial pressure of $Si(OH)_4$ increases by about 5 folds, and the other three species by two or more orders of magnitude when the temperature increases from 1200^{o}C to 1500^{o}C. In order to demonstrate the effect of the activity of SiO_2, partial pressures of these species are calculated at 1200^{o}C and 6 atm, one at $a_{SiO_2} = 1$ (directly exposure), and the other at $a_{SiO_2} = 0.05$ ($SrAS_2$ coating at 1200^{o}C).

These two calculations are compared in Figure 18, which clearly demonstrates that the partial pressure of every volatile species is reduced by more than one order of magnitude when $SrAS_2$ coating is used.

3.4 Discussions on the Limitations of the Approach

The purpose of this work is to integrate thermodynamic calculation with a gaseous-diffusion model to predict the volatility of SiO_2 as a function of combustion conditions and environmental barrier coating (EBC) materials. The prediction relies on the reliability of the thermodynamic database for the gas phase and the condensed phases of the EBC system, and the suitability of the gaseous-diffusion model. The accuracy of the Gibbs energy of every gas species, especially those volatile species, determines the predicted volatility of SiO_2 and the recession of SiC. As shown in Figure 3, the calculated weight loss rates of SiC are lower than those measured under fuel rich condition. One of the possible reasons is that other volatile species that are not considered in the database play a role. Therefore, a more comprehensive thermodynamic database, which includes the Gibbs energies of all possible gas species, is needed for more accurate predictions. Thermodynamic database for the EBC system, which is SrO-Al_2O_3-SiO_2 in this study, is essential since the activity of SiO_2 directly determines the partial pressures of volatile species and the volatility of SiO_2. This database needs to be extended to a higher order system if the modeling approach developed in this study is to be used for other coating materials. The gaseous-diffusion model used in this study was based on the assumption of laminar-flow conditions, and was used to calculate boundary layer diffusion controlled

fluxes. The major issue with this model is that in some circumstances, such as very high gas velocity, laminar flow is expected to give way to turbulent conditions, and the equations used in this study need to be corrected. The limitation of this model has been discussed by Opila *et al.* [5] and will not be repeated here. Although with limitations, the modeling approach developed with this study is a very useful tool in understanding the volatility of SiO_2 under a variety of combustion conditions, and different coating conditions.

4. CONCLUSION

A concept of integrating thermodynamic calculation with gaseous-diffusion model for the prediction of SiC recession caused by SiO_2 volatility under combustion conditions is successfully demonstrated in this study. In this approach, thermodynamic database for the gas phase and the condensed phase in the silica-oxide system is used to calculate the equilibrium between the selected EBC and the combustion environment. The calculated equilibrium partial pressures are then used by the gaseous-diffusion model to find the fluxes of volatile gas species and the weight loss of SiC resulted from the volatility of SiO_2. The advantage of this approach is that thermodynamic calculation is directly integrated with SiO_2 volatile kinetics and the activity effect of SiO_2 for a selected EBC can be instantly taken into account. As a result, the protective efficiency of different EBCs can be evaluated under a variety of combustion conditions, which provides a valuable guidance for the intelligent selection of EBCs for the SiC-based materials.

In this study, the volatility of SiO_2 and the recession of SiC under a variety of combustion conditions were calculated and compared favorably with the available experimental data. It is demonstrated that the SiC-based ceramics suffers significant weight loss when it was exposed to the combustion air directly, mullite ($3Al_2O_3 \cdot 2SiO_2$) coating reduces the SiC weight loss by about 50%, and $SrAS_2$ ($SrO \cdot Al_2O_3 \cdot 2SiO_2$) coating further prevents the SiC from recession. Two alloys: Sr_2AS ($2SrO \cdot Al_2O_3 \cdot SiO_2$) and $Sr_6A_9S_2$ ($6SrO \cdot 9Al_2O_3 \cdot 2SiO_2$), were identified as potential EBCs for SiC by our calculations. The even lower activity of SiO_2 in these two materials made them very promising coating materials for SiC. The effects of the equivalent ratio, temperature, and total pressure on the volatility of SiO_2 are also discussed. Temperature is found to have significant effects on the equilibrium partial pressures of the volatile species, and their fluxes. Higher temperature and/or higher pressure lead to heavier weight loss of SiC-based ceramics.

ACKNOWLEDGEMENTS

We would like to acknowledge the financial support from USAF due to a SBIR award: FA8650-09-M-5211 without which this work is not possible.

REFERENCES

1. K. N. Lee, D. S. Fox, and N.P. Bansal, *Rare earth silicate environmental barrier coatings for SiC/SiC composites and Si3N4 ceramics.* Journal of the European Ceramic Society, 2005. **25**: p. 1705-1715.

2. J. I. Federer, *Alumina base coating for protection of SiC ceramics.* J. Mater. Eng., 1990. **12**: p. 141-149.

3. J. R. Price, M. van Roode, and C. Stala, *Ceramic oxide-coated silicon carbide for high temperature corrosive environments.* Key Eng. Mater., 1992. **72-74**: p. 71-84.

4. K. N. Lee, R. A. Miller, and N. S. Jacobson, *New generation of plasma-sprayed mullite coatings on silicon-carbide.* J. Am. Ceram. Soc., 1995. **78**(3): p. 705-710.

5. E. J. Opila, et al., *SiC Recession Caused by SiO2 Scale Volatility under Combustion Conditions: II, Thermodynamics and Gaseous-Diffusion Model.* J. Am. Ceram. Soc., 1999. **82**(7): p. 1826-1834.

6. R. C. Robinson and J.L. Smialek, *SIC Recession Caused by SiO2 Scale Volatility under Combustion Conditions: I, Experimental Results and Empirical Model.* J. Am. Ceram. Soc., 1999. **82**(7): p. 1817-1825.

7. E. J. Opila and R. E. Hann, *Paralinear Oxidation of CVD SiC in Water Vapor.* J. Am. Ceram. Soc., 1997. **80**(1): p. 197-205.

8. W. M. Kays and M. E. Crawford, *Convective Heat and Mass Transfer*. 1980, New York: McGraw-Hill.

9. R. A. Svehla, *Estimated Viscosities and Thermal Conductivities of Gases at High Temperatures*. 1962, NASA Glenn Research Center.

10. G. H. Geiger and D. R. Poirier, *Transport Phenomena in Metallurgy*. 1973, Reading, MA: Addison-Wesley.

11. *NIST-JANAF Thermochemical Tables*. Fourth ed, ed. M.W. Chase. 1998, New York: the American Chemical Society and the American Institute of Physics for the National Institute of Standards and Technology.

12. Zhang, C., Zhang, F., Cao, W.-S., and Chang Y. A., *Thermodynamic Modeling of the Al-Si-Sr-O System.* Intermetallics, 2009. **under review**.

13. *Pandat - Phase diagram calculation software package for multicomponent systems*. 2000, CompuTherm, LLC: Madison, WI 53719.

14. Bowen, N.L., Greig, J.W., *The System: Al2O3.* J. Am. Ceram. Soc., 1924. **7**(4): p. 238-254.

15. Toropov, N.A., Galakhov, F.Y., *New Data on the System Al2O3-SiO2.* Dokl. Akad. Nauk. S.S.S.R, 1951. **78**(2): p. 299-302.

16. Konopicky, K., *Equilibrium Diagram of the System SiO2-Al2O3.* Bull. Soc. Franc. Ceram., 1956. **33**: p. 3-6.

17. Aramaki, S., Roy, R., *Revised Equilibrium Diagram for the System Al2O3-SiO2.* J, Am. Ceram. Soc., 1962. **45**(5): p. 229-242.

18. Davis, R.F., Pask, J.A., *Diffusion and Reaction Studies in the System Al2O3-SiO2.* J, Am. Ceram. Soc., 1972. **55**(10): p. 525-531.

19. Aksay, I.A., Pask, J.A. , *Stable and Metastable Equilibria in the System SiO2-Al2O3.* J, Am. Ceram. Soc., 1975. **58**(11-1): p. 507-512.

20. Prochazka, S., Klug, F.J., *Infrared-Transparent Mullite Ceramic.* J, Am. Ceram. Soc., 1983. **66**(12): p. 874-880.

21. Hamano, K., Sato, T., Nakagawa, Z., *Properties of Mullite Powder Prepared by Coprecipitation and Microstructure of Fired Bodies.* Yogyo Kyokaishi, 1986. **94**(8): p. 818-822.

22. Klug, F.J., Prochazka, S. Dorrmus, R.H., *Alumina-Silica Phase Diagram in the Mullite Region.* J, Am. Ceram. Soc., 1987. **70**(10): p. 750-759.

23. Okada, K., Otsuka, N., *Change in Chemical-Composition of Mullite Formed from 2SiO2.3Al2O3 Xerogel During the Formation Progress.* J, Am. Ceram. Soc., 1987. **70**(10): p. 245-247.

24. Dear, P.S., *Sub-liquidus equilibria for the ternary system SrO-Al_2O_3-SiO_2.* Bulletin of the Virgina Polytechnic Institute, 1957. **L**(11): p. 1-12.

Table I: Experimental conditions of Robinson *et al.* [6]

Fuel Condition	T (^{o}C)	P (atm)	V_g (m/s)	Equivalence Ratio
Fuel rich	1225-1450	6-6.3	18-24	1.69-1.97
Fuel lean	1200-1450	6-6.3	20-23	0.87-0.94
Fuel lean	1295-1420	10	18-19	0.76-0.87

Table II: Calculation conditions used in this work

Fuel Condition	T (^{o}C)	P (atm)	Vg (m/s)	Equivalence Ratio	Constants
Fuel rich	1200-1500	6	21	1.8	$\eta=5.179\times10^{-4}$ (g/cm·s) D=0.287 cm^2/s
Fuel lean	1200-1500	6	21	0.9	
Fuel lean	1200-1500	10	18.5	0.8	

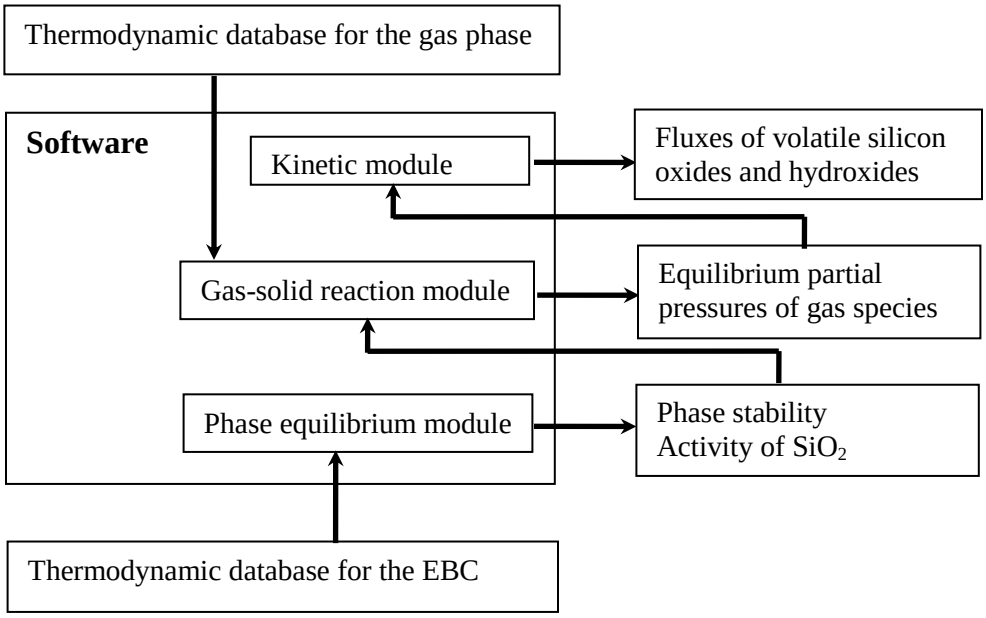

Figure 1**:** Flow chart that shows the connection of different modules of the software and the databases

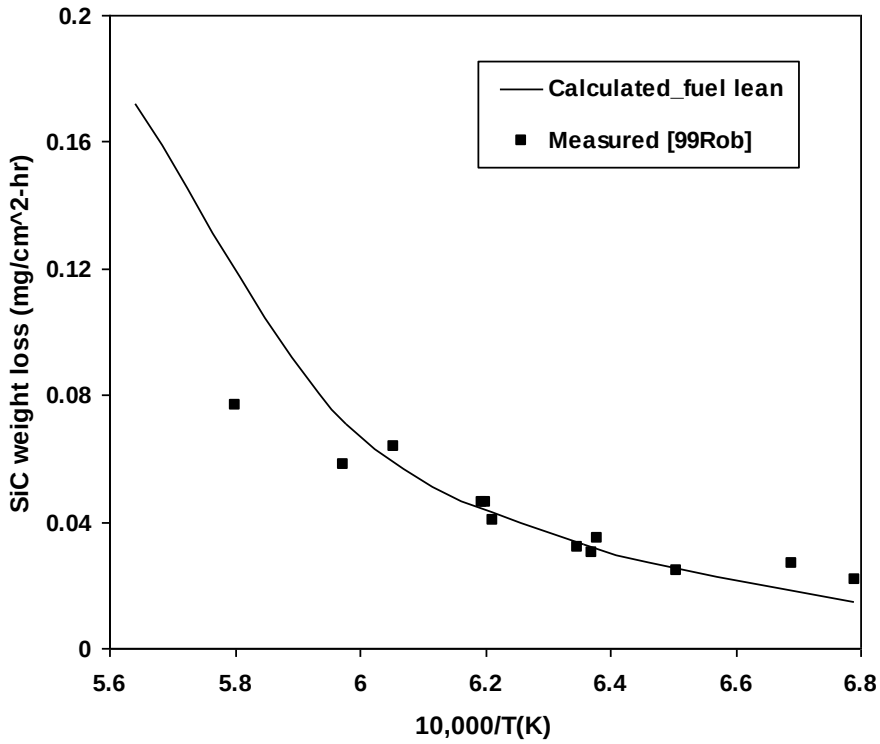

Figure 2: Comparison between the calculated and measured SiC weight loss rate under fuel lean condition at 6 atm (Table II)

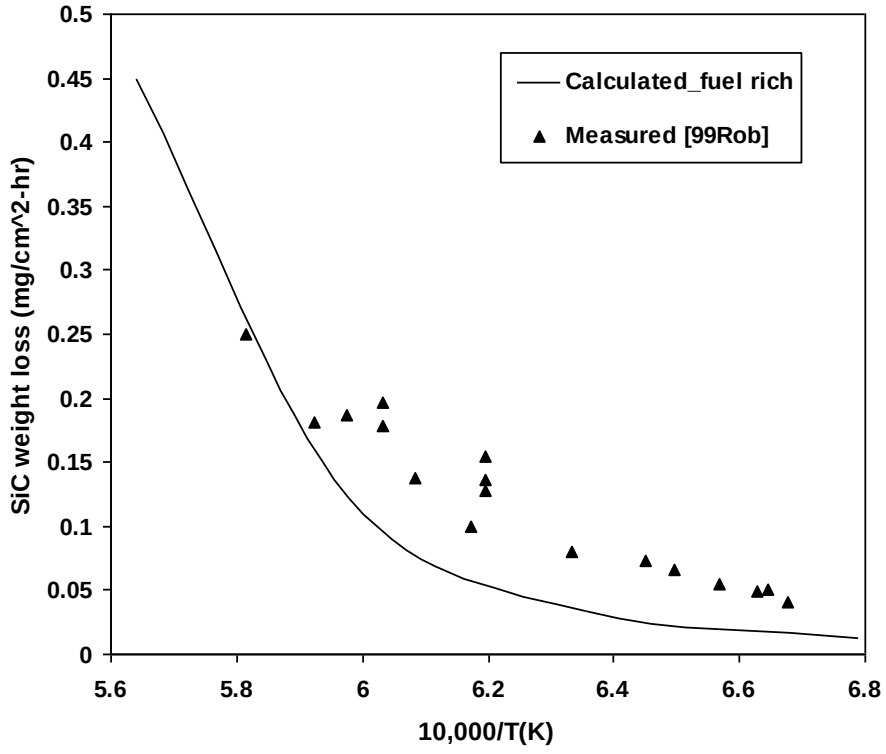

Figure 3: Comparison between the calculated and measured SiC weight loss rate under fuel rich condition at 6 atm (Table II)

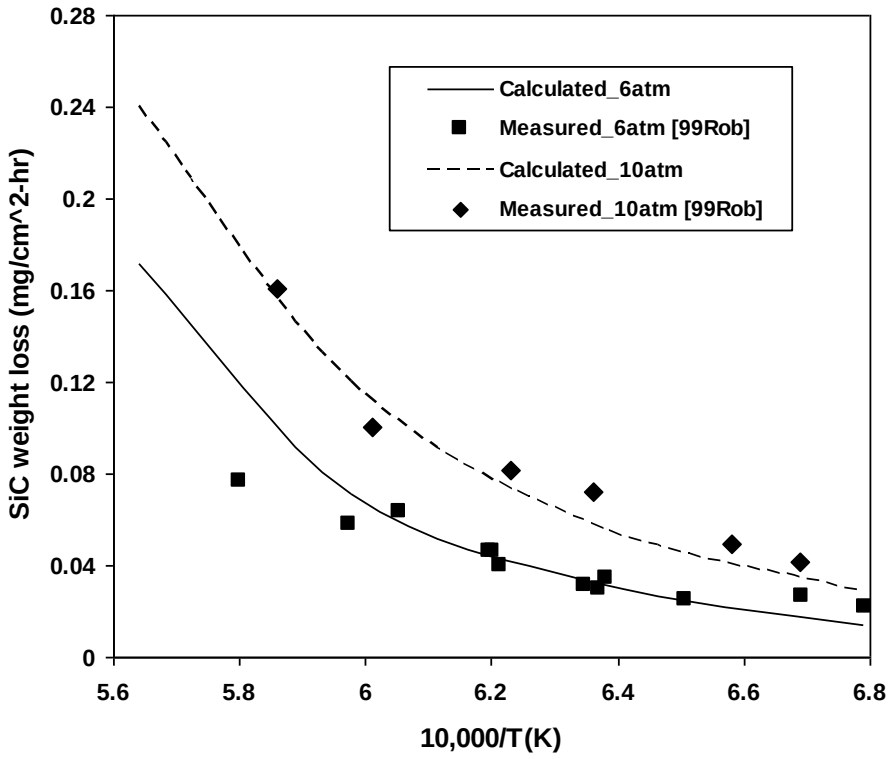

Figure 4: Comparison between the calculated and measured SiC weight loss rate under fuel lean condition at two different pressures (Table II)

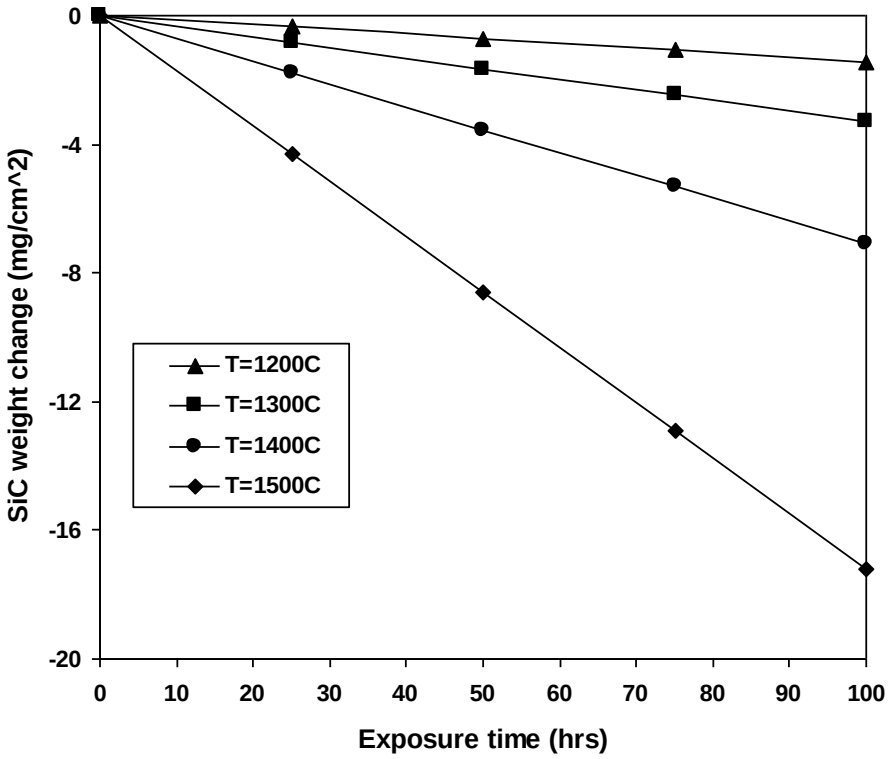

Figure 5: Effect of temperature on the weight loss of SiC at P = 6 atm

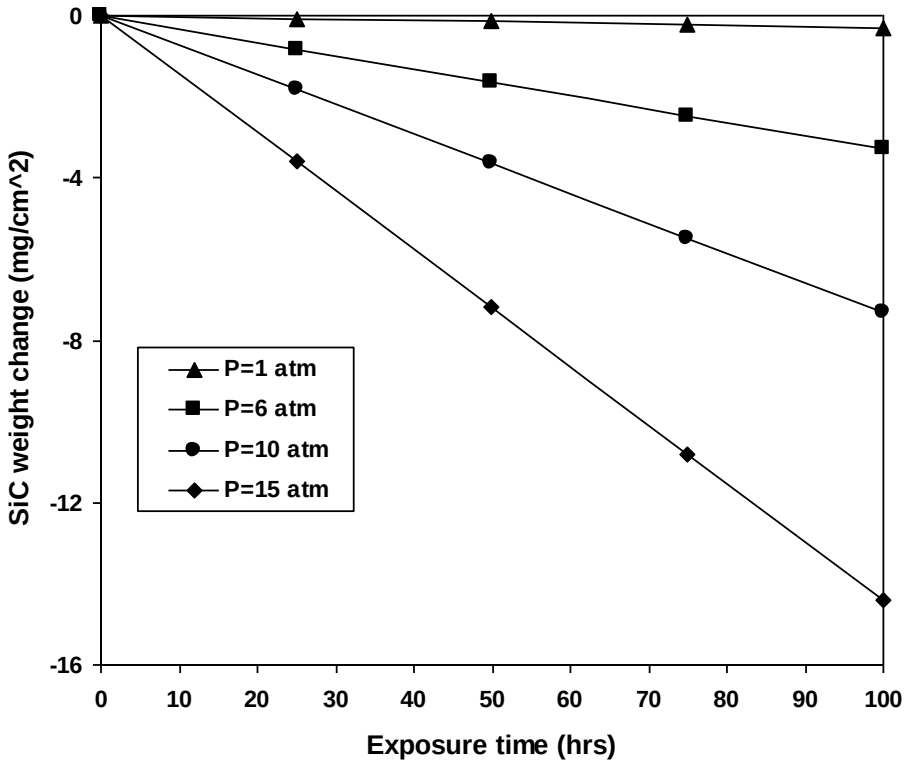

Figure 6: Effect of combustion air pressure on the weight loss of SiC at T = 1300^{o}C

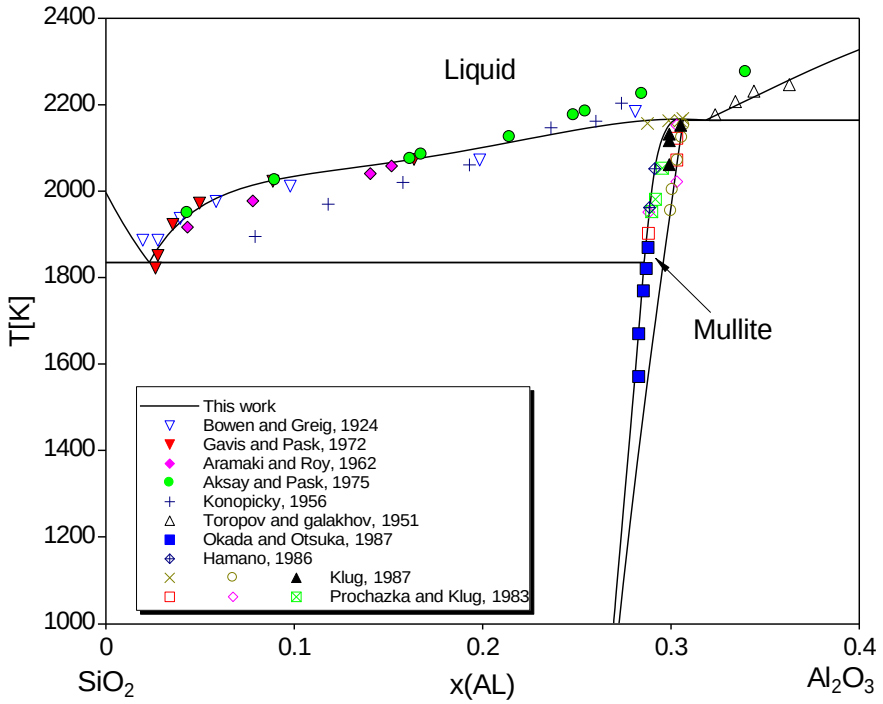

Figure 7: Calculated SiO_2-Al_2O_3 phase diagram along with the experimental data from literatures [14-23]

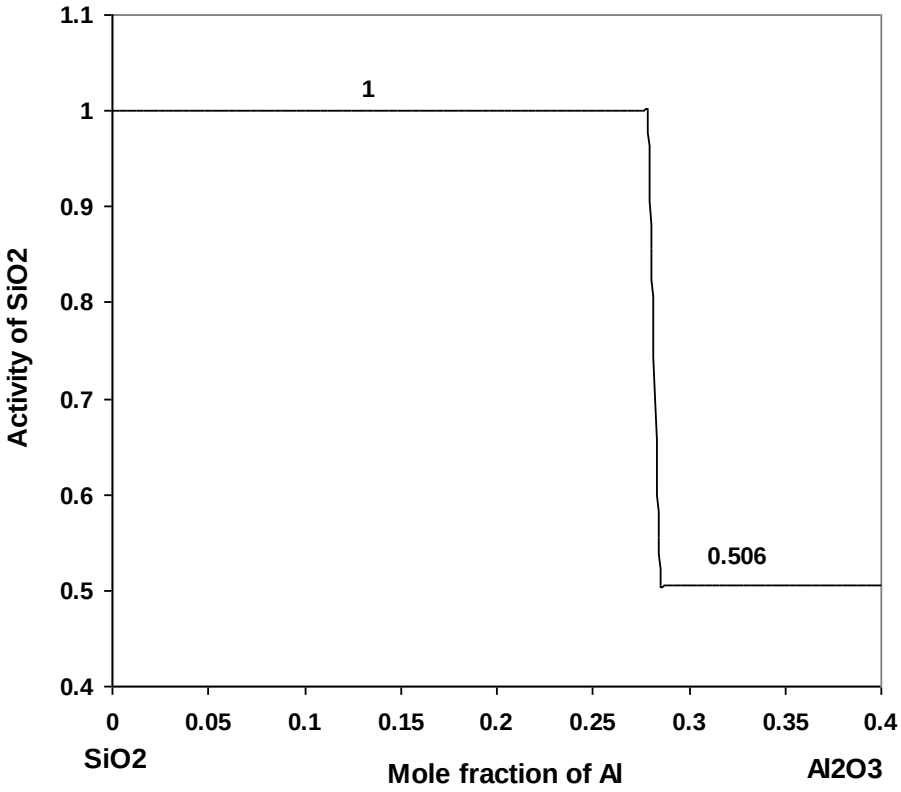

Figure 8: Activity of SiO_2 along the SiO_2-Al_2O_3 pseudo-binary at T = 1500K

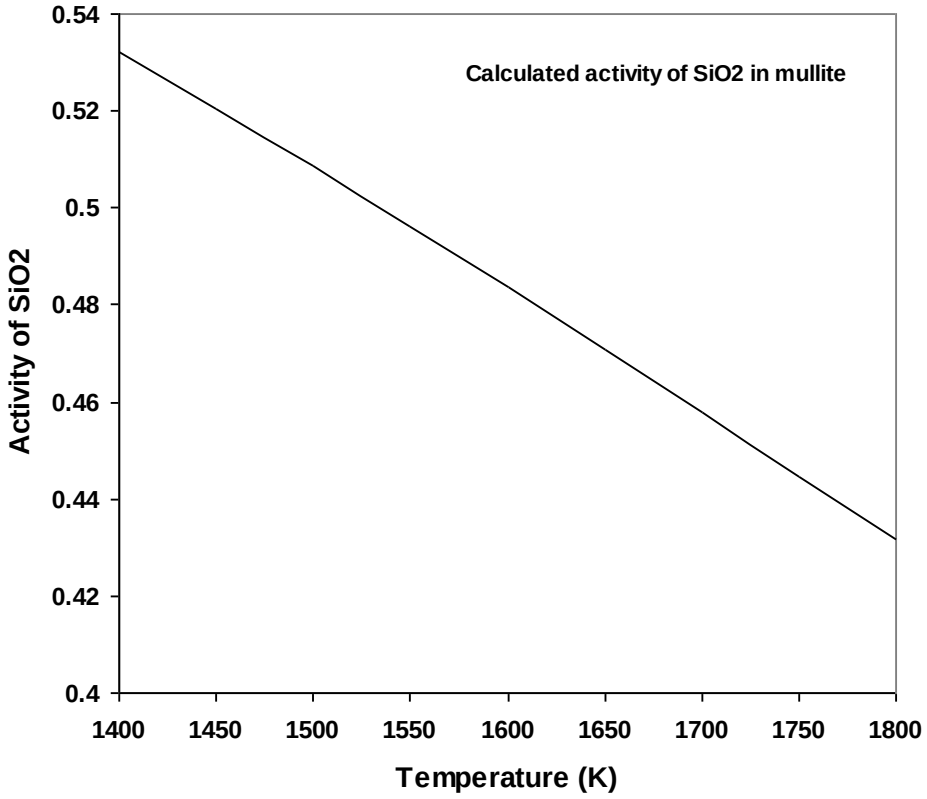

Figure 9 : Activity of SiO_2 as a function of temperature along the mullite/mullite+Al_2O_3 phase boundary

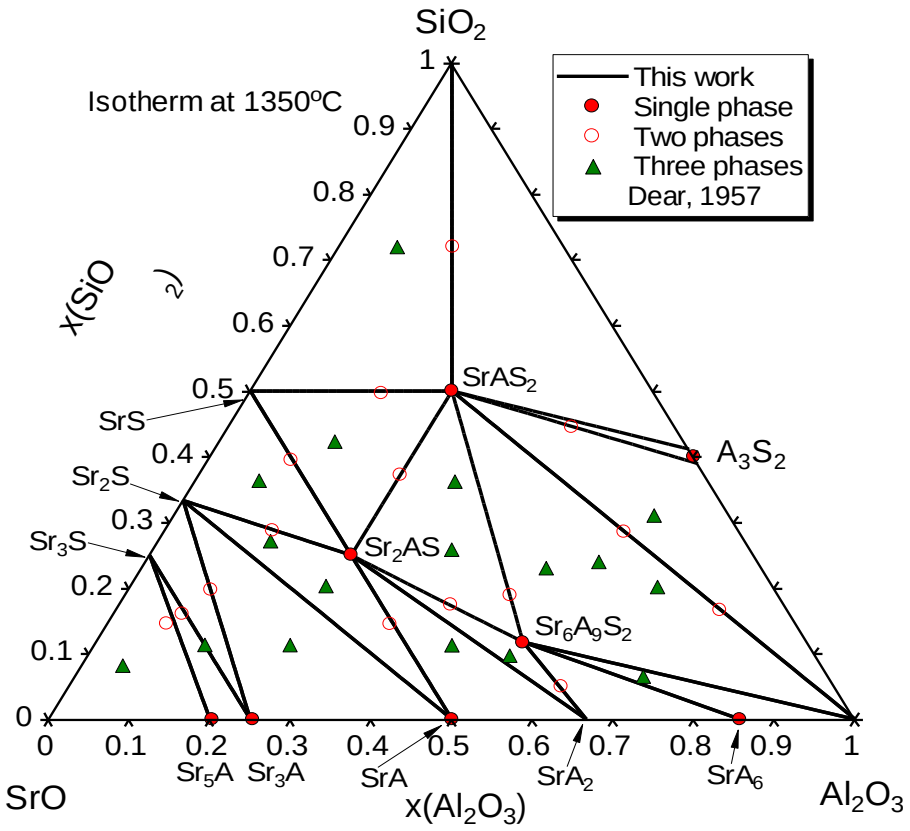

Figure 10: Calculated isothermal section for the SrO-Al_2O_3-SiO_2 pseudo-ternary system at 1350°C along with the experimental data from Dear *et al.* [24]

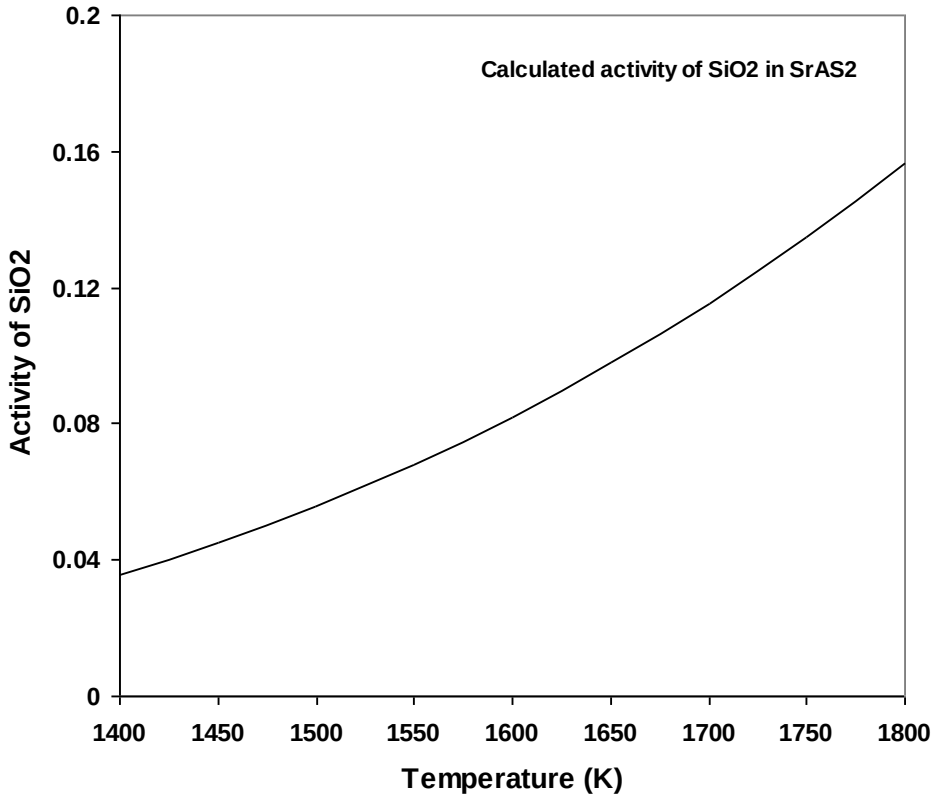

Figure 11: Activity of SiO_2 in $SrAS_2$ ($SrO{\cdot}Al_2O_3{\cdot}2SiO_2$) as a function of temperature

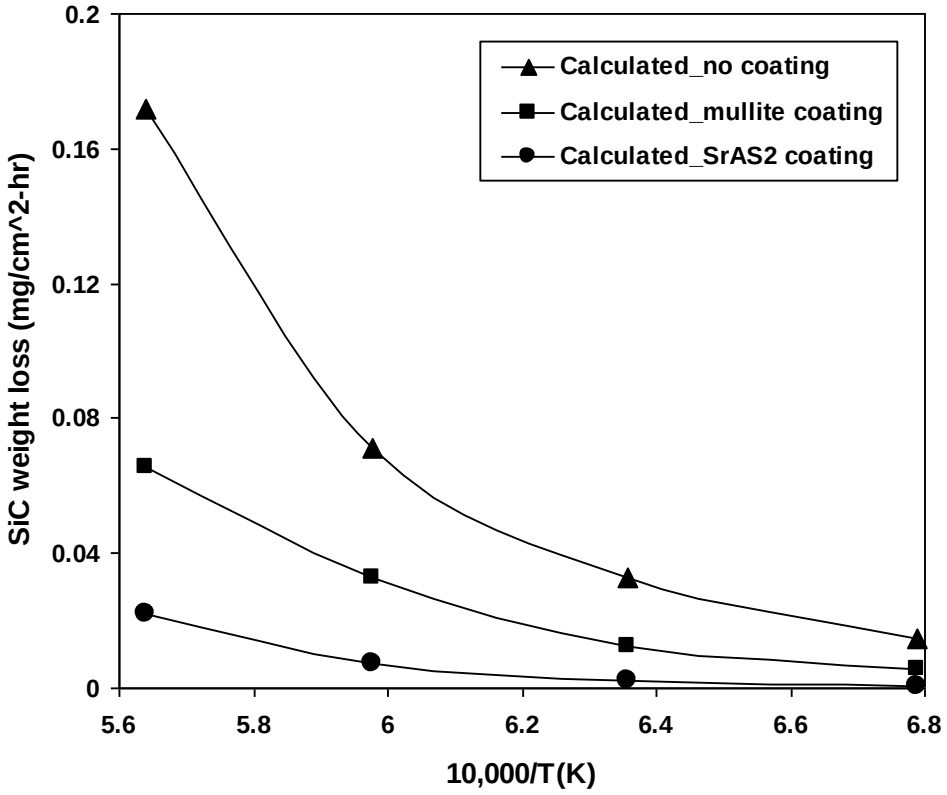

Figure 12: Calculated weight loss rate of SiC under three conditions: no coating, mullite coating and $SrAS_2$ coating

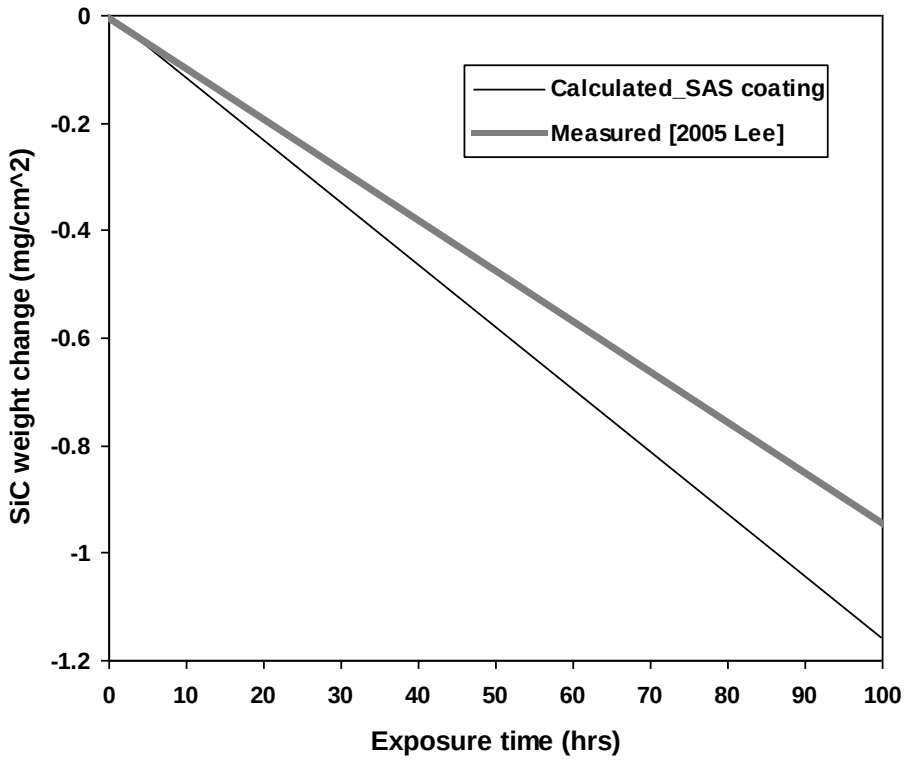

Figure 13: Comparison between the calculated and measured SiC weight loss [1] when $SrAS_2$ coating is used

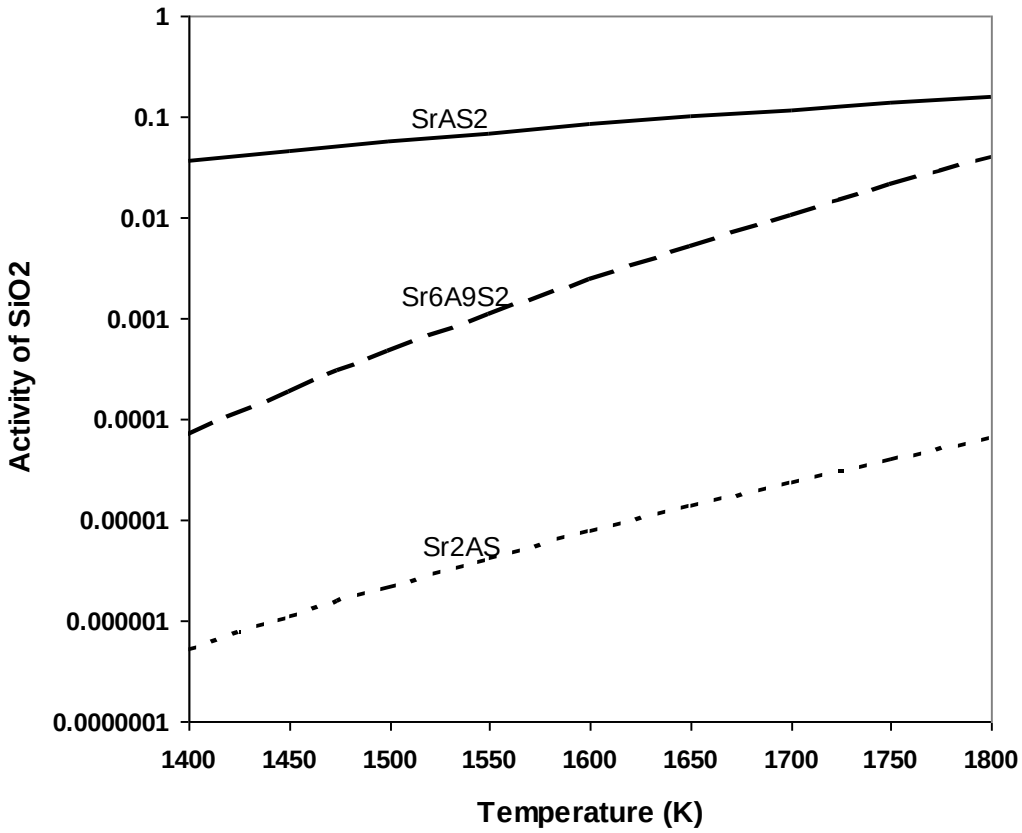

Figure 14: Comparison of activity of SiO_2 in $SrAS_2$, Sr_2AS, and $Sr_6A_9S_2$ as a function of temperature

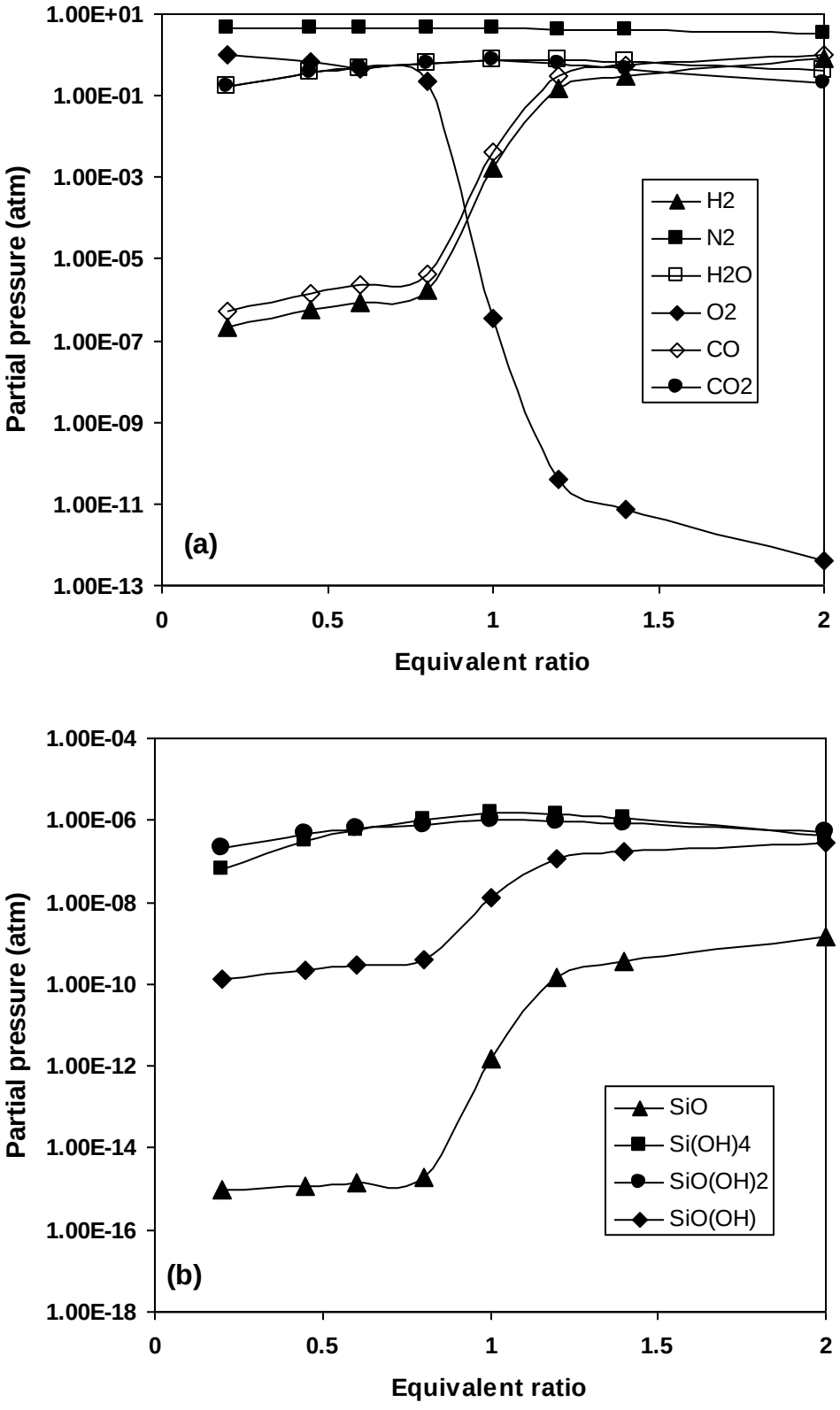

Figure 15: Partial pressure of gas species at 1200^{o}C and a total pressure of 6 atm

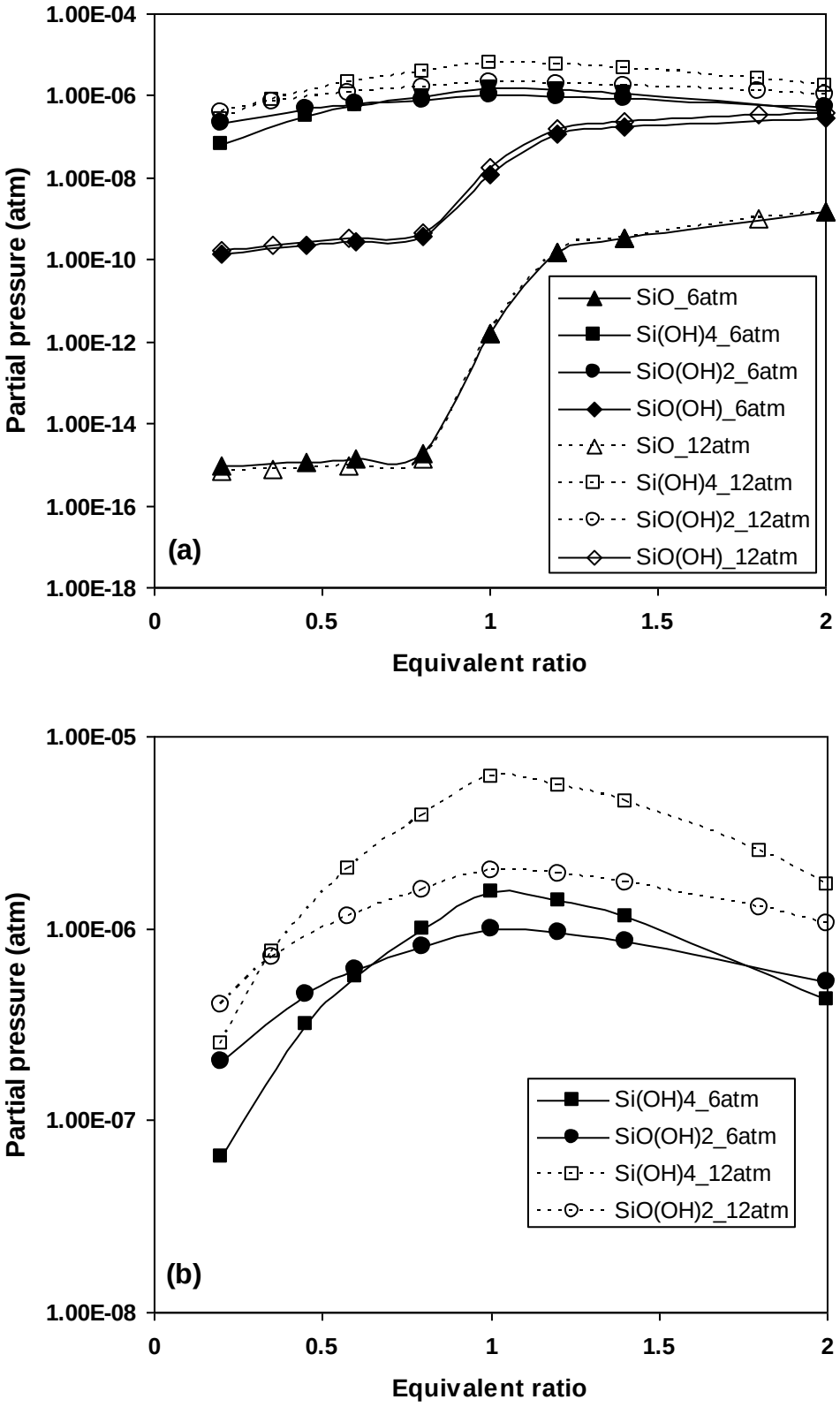

Figure 16: Partial pressure change of volatile species with the total pressure at T=1200^{o}C

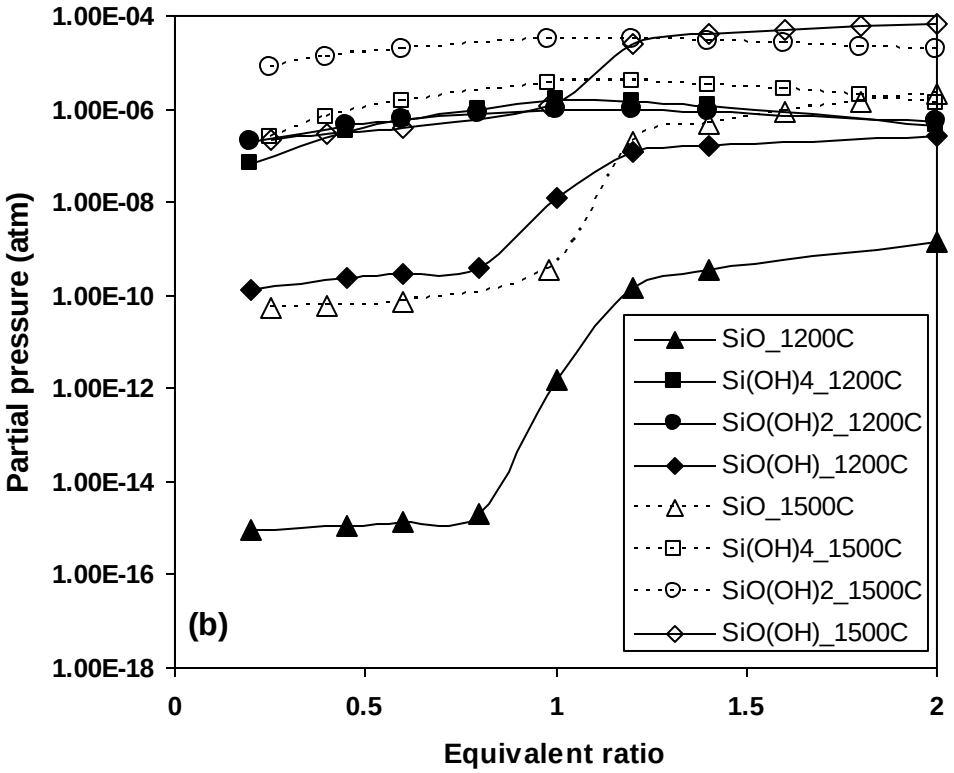

Figure 17**:** Partial pressure change of volatile species with temperature at P=6 atm

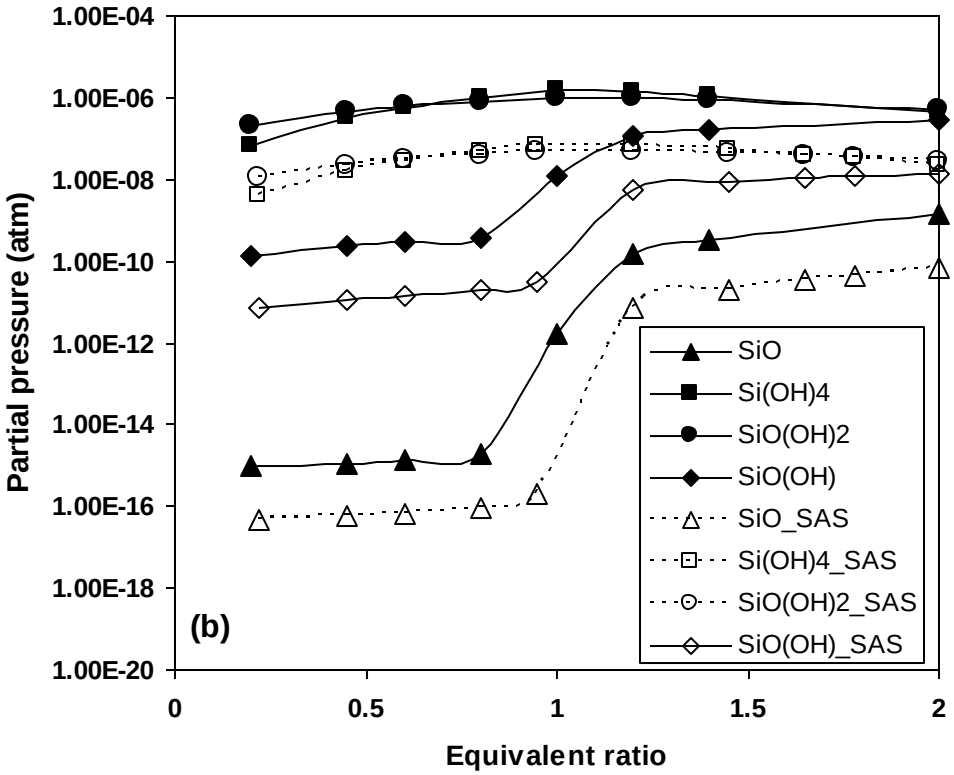

Figure 18: Effect of the activity of SiO_2 (with or without coating) on the partial pressures of the volatile species at T=1200^{o}C and P=6 atm